15th World Congress on Computational Mechanics (WCCM-XV)
8th Asian Pacific Congress on Computational Mechanics (APCOM-VIII)
Virtual Congress: 31 July – 5 August 2022
S. Koshizuka (Ed.)

NUMERICAL EVALUATION OF BELL-SHAPED PROPORTIONAL DAMPING MODEL FOR SOFTENING STRUCTURES

CHIN-LONG LEE[1] AND THEODORE L. CHANG[2]

[1] University of Canterbury
69 Creyke Road, Christchurch 8041, New Zealand
chin-long.lee@canterbury.ac.nz

[2] IRIS Adlershof der Humboldt-Universität zu Berlin
Zum Großen Windkanal 2, Berlin 12489, Germany
tlcfem@gmail.com

Key words: Proportional Damping, Bell-Shaped Model, Softening Response, Negative Stiffness

Abstract. *A new type of proportional damping models, called bell-shaped proportional damping model, has recently been proposed. This new model has not only addressed the spurious damping forces, but also maintained the same order of computational efficiency as the Rayleigh model. This model has also been further improved such that, by using the tangent stiffness approach, it becomes suitable for structures experiencing softening response with negative stiffness. The improved model allows users to have flexible control of modal damping ratio for all interested frequency intervals, including those associated with negative stiffness. In this study, the performance of bell-shaped damping model is evaluated numerically in a response history analysis of a multi-storey building under seismic loading. The results show that, compared to the Rayleigh model, the bell-shaped model performs excellently in terms of always giving desirable positive energy dissipation even when the structure is experiencing softening response.*

1 INTRODUCTION

In the modeling of large-scale structures subjected to earthquake ground motions, energy dissipation not already accounted for using material hysteretic models in structural components, often called unmodeled damping, are usually incorporated using viscous damping such as Rayleigh damping [1] due to mathematical convenience and computational efficiency. The use of the Rayleigh damping model during inelastic response after yielding occurs could, however, lead to large spurious damping forces in the order comparable to material constitutive forces. This problem has been well-documented and studied [e.g. 2–8].

Many remedies have been proposed to eliminate the spurious damping forces [e.g. 6, 9–13]. However, most of them are not computationally efficient, and some also deviate from the idea of modal damping ratio due to loss of proportionality, resulting in difficulty for model parameter calibration against experimentally measured modal damping ratios. Most models are also not suitable for structures experiencing softening response due to having negative damping ratio.

In a recent study, a new type of proportional damping model, called *bell-shaped*, has been proposed [14–20], which has been shown to address most of the issues in the current damping models discussed above. In particular, it maintains positive damping using the tangent stiffness approach where the damping coefficient matrix is proportional to the tangent stiffness of the structure. In this study, this great feature of the bell-shaped damping model will be evaluated by simulating the seismic response of a realistic inelastic multi-storey building structure that experiences softening response with negative stiffness, with the focus on examining the time history of accumulated viscous energy dissipation.

2 BELL-SHAPED DAMPING MODEL

The bell-shaped damping model is first briefly introduced in the following. It uses a bell-shaped curve (with a peak value of 1 at frequency ω_p) in the frequency domain, see Fig. 1, as a basis function N of normalized frequency $\omega_r = \omega/\omega_p$ to generate arbitrary user-defined damping ratio curves by combining several scaled basis functions. Examples include uniform, linear and trilinear curves [14, 16]. It can

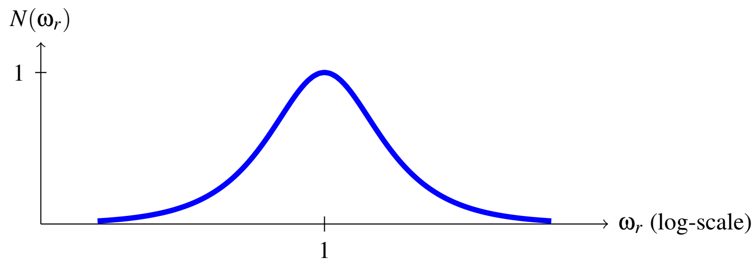

Fig. 1: Damping ratio curve of bell-shaped damping model.

be implemented as a sparse matrix [15, 17], maintaining the same order of computational cost as the Rayleigh model, making it suitable for structures with a large number of degrees of freedom. It has also been further improved with several variants: Types 1, 2 and 3 [18, 19], allowing the frequency bandwidth of the basis function to be adjusted in order to match a curve with drastic changes across a small frequency interval, where a particular example is a step distribution.

With its great flexibility in generating a damping ratio curve that covers a broad range of frequencies of interests, the bell-shaped damping model opens up great potential in simulating energy dissipation using tangent stiffness approach, where the damping coefficient matrix follows the tangent stiffness matrix, allowing damping ratio and rate of energy dissipation during inelastic response to be prescribed as well. Some showed concerns about this approach, particularly that it could lead to negative damping ratios when the structure being modeled is experiencing softening response with negative stiffness. These concerns have been largely addressed recently [20]. An improved bell-shaped damping model, called Type 4, has also been proposed in the same study [20] to ensure no negative damping ratio during the softening response. This improved damping model has two bell-shaped curves, with one at each side of the vertical axis, in its basis function N_4. See Fig. 2 for some examples of the new basis function. The one on the right side of the vertical axis corresponds to the positive signed frequencies ($l\omega_r > 0$, l: sign of stiffness) associated with positive stiffness, while the one on the left side corresponds to those associated with negative stiffness. The height of the left bell curve can also be adjusted up and down with suitable parameter values. More information on setting the parameter values can be found in the previous work [20]. This provides users with flexibility to specify damping ratios for frequencies of negative stiffness different from those of positive stiffness.

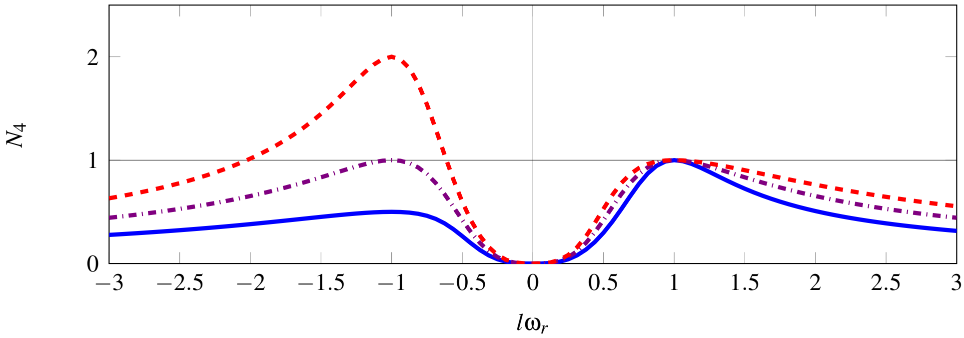

Fig. 2: Examples of Type 4 basis function.

3 PERFORMANCE EVALUATION

The structural model considered in the performance evaluation is a steel moment resistant frame slightly modified from an SAC model [21]. It has three storeys, two bays, and one gravity column (see Fig. 3). The section names of beams and columns are shown in the figure. The total horizontal

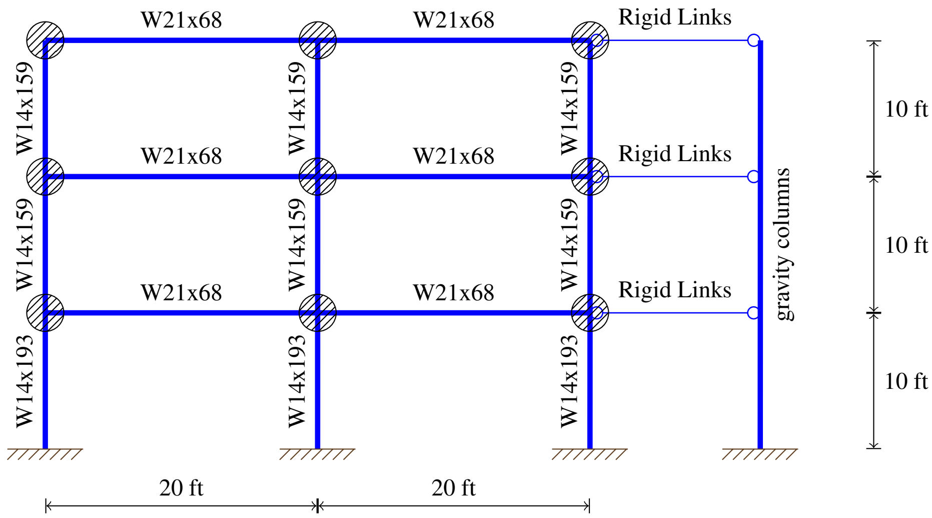

Fig. 3: Numerical model of case study structure (modified from an SAC model).

mass at each floor distributed to this frame is 1.25 kips-sec-sec/in. It is lumped at nodes based on their tributary areas. The vertical mass on the moment-resisting frame is one-sixth of the horizontal mass. The Young's modulus of the steel material is 29,000 ksi, and the yield strength is 50 ksi. At each floor, the gravity loads are applied such that 80.44 kips are applied to the steel moment resisting frame, distributed to each node based on their tributary areas, and 402.2 kips are applied to the gravity column. The first three elastic frequencies of the structure are 1.22 Hz, 4.24 Hz and 8.02 Hz.

All beams and columns are modeled using the plastic hinge element prescribed with a yield surface considering N-M interaction [22, 23]. To simulate the effect of softening response, a value of -0.05 is assigned to the kinematic hardening parameter K, which will result in about 8% softening stiffness relative to the elastic case. The second order P-Δ effects are simulated using the corotational formulation.

A 2% damping is assumed for a wide range of frequencies between 0.01 Hz and 100 Hz. The same amount of damping is also assumed for the range of frequencies associated with the negative stiffness case. The damping ratio curve corresponding to this distribution in the structural frequency f_n (Hz) domain is shown in Fig. 4 on the symmetric log scale generated using `symlog` [24]. The damping ratio

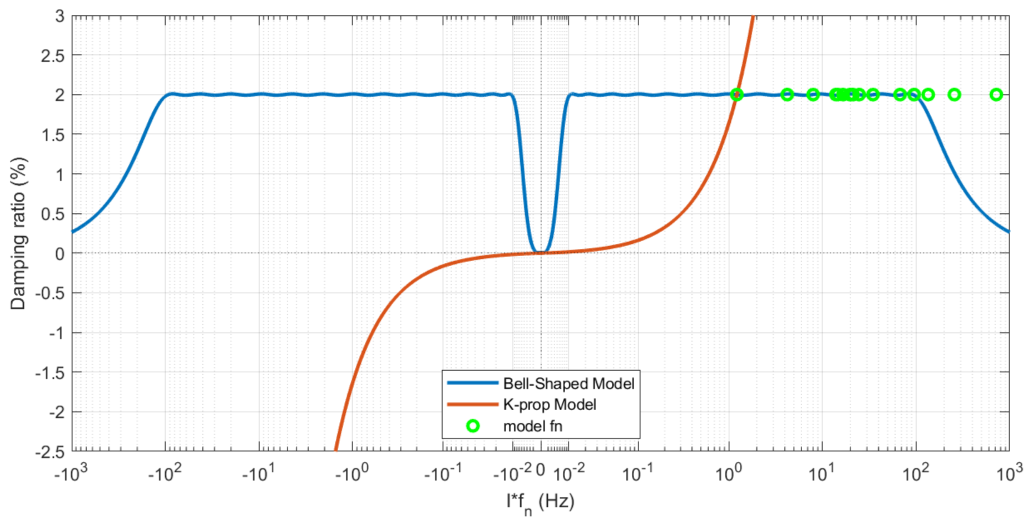

Fig. 4: The damping ratio curve assumed in the model.

curve is generated using thirteen basis functions of Type 2 bell-shaped model. The relative error of the damping ratio within the frequency interval is less than 1%.

The curves on the right side of the vertical axis show the damping ratio for the frequencies associated with positive stiffness, while the curves on the left side show those associated with negative stiffness, indicated by the signed of the stiffness l. The damping ratio curve generated using the Rayleigh model with only the stiffness proportional term is also shown for comparison. It matches a 2% damping for the first mode only. The damping ratio increases linearly (shown nonlinearly on the symmetric log scale) with the frequencies of other modes. It shows negative damping whenever the structural frequency is less than zero.

The input ground motion is the North-South component of the recorded 1940 El Centro earthquake. The motion was doubled such that its peak ground acceleration is about 0.7 g in order to cause major damages to the structure. The simulation was conducted using the software `suanPan` [25], which has the bell-shaped damping model implemented.

4 RESULTS AND DISCUSSIONS

The time histories of roof drifts (displacements normalized by the building height) are shown in Fig. 5. As shown, the roof drifts show long-duration residuals due to accumulated inelastic damages. The drifts

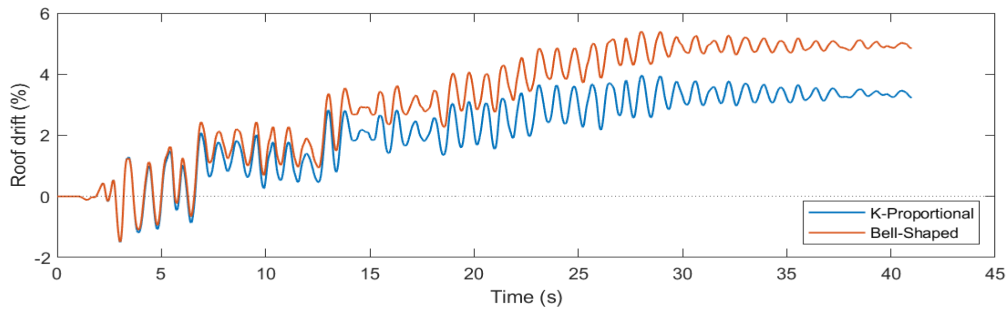

Fig. 5: Roof drifts.

using the stiffness-proportional damping are shown to be smaller than that using the bell-shaped model for the following reasons:

- Due to having infinite damping ratio at infinite frequency, the stiffness-proportional model would always result in spurious damping forces whenever yielding occurs [8, 16].
- Compared to the bell-shaped model, the stiffness proportional model gives a higher damping ratio for higher modes, resulting in higher damping forces in general.

The base shear versus roof drift relationship experienced by the building is shown in Fig. 6. As shown

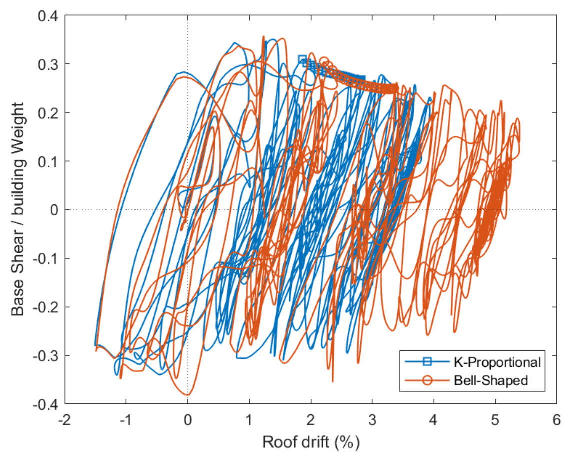

Fig. 6: Base shear versus roof displacement hysteresis (softening response highlighted with markers).

in this figure, the base shear exhibits softening response when the roof drift exceeds 1%, particularly during the time interval between 12.8 sec and 13 sec, where the response are highlighted with markers shown in the figure. This softening response results in having a global negative stiffness in the structure. It would be of great interest to know if viscous damping is always maintained as positive so that no unwanted energy is added to the system.

Fig. 7 shows the accumulated energy dissipation due to the viscous damping over the whole duration of building response on the left side, and the energy dissipation increment or rate ($\approx \Delta\text{Energy}/\Delta t$) for the time interval between 12.8 sec and 13 sec on the right side. In general, the stiffness proportional

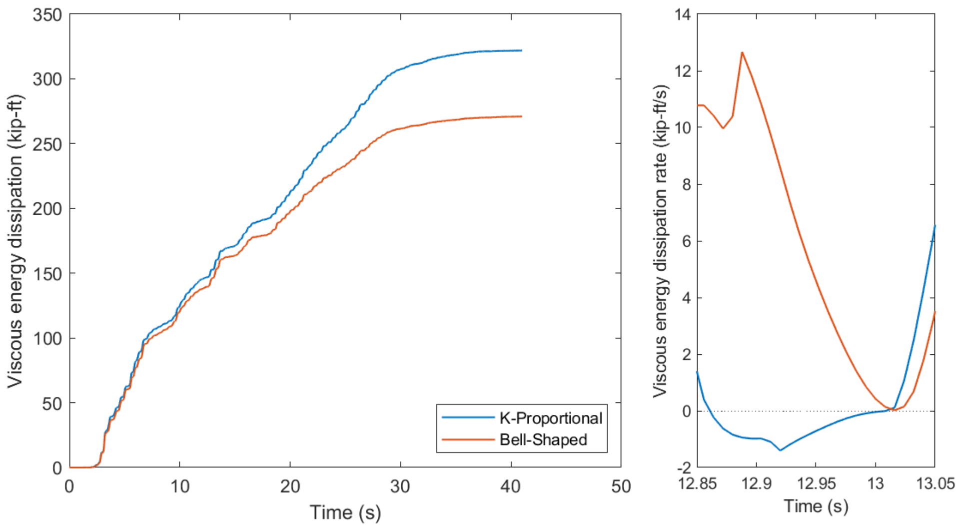

Fig. 7: Base shear versus roof displacement hysteresis.

model gives a larger energy dissipation because it has a relatively larger damping ratio for all but the first mode. At the first glance, both damping models give an expected increasing accumulated viscous energy dissipation. However, a closer look into the rate of energy dissipation for the time interval between 12.8 sec and 13 sec shows that the stiffness proportional model did give negative damping increment during this time interval. It will result in adding energy to the system, which is contrary to the need of introducing the viscous damping to the system. This negative damping is unacceptable. Note, the value of this negative damping is small because it is a total energy dissipation contributed by all the modes, including those with positive damping, which might have overshadowed those modes with negative damping. On the other hand, the bell-shaped model maintained positive damping during this time interval, confirming this feature of the bell-shaped model.

5 CONCLUSIONS

In this study, the performance of a newly proposed bell-shaped model has been evaluated by simulating the seismic response of a realistic multi-storey SAC building model. The numerical results have shown that the bell-shaped model can maintain positive damping even when the structure experiences softening response with negative stiffness. This feature is superior to the stiffness proportional model that resulted in having negative damping when stiffness is negative, as demonstrated in the example.

REFERENCES

[1] Rayleigh, J. W. S. B. *The theory of sound*, vol. 2 (Macmillan, 1896).

[2] Chrisp, D. J. *Damping models for inelastic structures*. Master's thesis, University of Canterbury, Christchurch, New Zealand (1980).

[3] Léger, P. & Dussault, S. Seismic-energy dissipation in MDOF structures. *Journal of Structural Engineering* **118**, 1251–1269 (1992).

[4] Bernal, D. Viscous damping in inelastic structural response. *Journal of Structural Engineering*

120, 1240–1254 (1994).

[5] Carr, A. Damping models for inelastic analyses. In *Proceedings of the Asia-Pacific vibration conference*, 42 (Kyongju, Korea, 1997).

[6] Hall, J. F. Problems encountered from the use (or misuse) of Rayleigh damping. *Earthquake engineering & structural dynamics* **35**, 525–545 (2006).

[7] Charney, F. A. Unintended consequences of modeling damping in structures. *Journal of structural engineering* **134**, 581–592 (2008).

[8] Chopra, A. K. & McKenna, F. Modeling viscous damping in nonlinear response history analysis of buildings for earthquake excitation. *Earthquake Engineering & Structural Dynamics* **45**, 193–211 (2016).

[9] Puthanpurayil, A. M., Lavan, O., Carr, A. J. & Dhakal, R. P. Elemental damping formulation: an alternative modelling of inherent damping in nonlinear dynamic analysis. *Bulletin of Earthquake Engineering* **14**, 2405–2434 (2016).

[10] Hall, J. F. Performance of viscous damping in inelastic seismic analysis of moment-frame buildings. *Earthquake Engineering & Structural Dynamics* **47**, 2756–2776 (2018).

[11] Lanzi, A. & Luco, J. E. Elastic velocity damping model for inelastic structures. *Journal of Structural Engineering* **144**, 04018065 (2018).

[12] Huang, Y., Sturt, R. & Willford, M. A damping model for nonlinear dynamic analysis providing uniform damping over a frequency range. *Computers & Structures* **212**, 101–109 (2019).

[13] Salehi, M. & Sideris, P. Enhanced Rayleigh damping model for dynamic analysis of inelastic structures. *Journal of Structural Engineering* **146**, 04020216 (2020).

[14] Lee, C.-L. A novel damping model for earthquake induced structural response simulation. In *Proceedings of the 2019 Pacific Conference on Earthquake Engineering and Annual NZSEE Conference*, 4C.07 (Auckland, New Zealand, 4-6 April 2019).

[15] Lee, C.-L. Efficient proportional damping model for simulating seismic response of large-scale structures. In Papadrakakis, M. & Fragiadakis, M. (eds.) *COMPDYN 2019 Proceedings*, vol. 3, 4557–4564 (2019).

[16] Lee, C.-L. Proportional viscous damping model for matching damping ratios. *Engineering Structures* **207**, 110178 (2020).

[17] Lee, C.-L. Sparse proportional viscous damping model for structures with large number of degrees of freedom. *Journal of Sound and Vibration* 115312 (2020).

[18] Lee, C.-L. Proportional viscous damping model for matching frequency-dependent damping ratio. In *17th world conference in earthquake engineering*, 2k–0043 (Sendai, 2020).

[19] Lee, C.-L. Bell-shaped proportional viscous damping models with adjustable frequency bandwidth. *Computers & Structures* **244**, 106423 (2021).

[20] Lee, C.-L. Type 4 bell-shaped proportional damping model and energy dissipation for structures with inelastic and softening response. *Computers & Structures* **258**, 106663 (2022).

[21] FEMA. State of the art report on systems performance of steel moment frames subjected to earthquake ground shaking. Tech. Rep. FEMA-355C, Federal Emergency Management Agency, Washington, D.C. (2000).

[22] Kostic, S. M., Filippou, F. C. & Lee, C.-L. An efficient beam-column element for nonlinear 3D frame analysis. In Papadrakakis, M., Fragiadakis, M. & Plevris, V. (eds.) *ECCOMAS Thematic Conference - COMPDYN 2011: 3rd International Conference on Computational Methods in Structural Dynamics and Earthquake Engineering: An IACM Special Interest Conference, Programme*

(Corfu, Greece, 2011).

[23] Kostic, S. M., Filippou, F. C. & Lee, C.-L. An efficient beam-column element for inelastic 3D frame analysis. In Papadrakakis, M., Fragiadakis, M. & Plevris, V. (eds.) *Computational Methods in Earthquake Engineering: Volume 2*, 49–67 (Springer Netherlands, Dordrecht, 2013).

[24] Perrotta, R. symlog (2022). URL `https://github.com/raaperrotta/symlog`. Https://github.com/raaperrotta/symlog, accessed on 26 April 2022.

[25] Chang, T. L. suanpan — an open source, parallel and heterogeneous finite element analysis framework (2022). URL `https://github.com/TLCFEM/suanPan`. Https://doi.org/10.5281/zenodo.6108919.